SPANDIDOS PUBLICATIONS

ONCOLOGY LETTERS 18: 2763-2770, 2019

# Combination value of diffusion-weighted imaging and dynamic susceptibility contrast-enhanced MRI in astrocytoma grading and correlation with GFAP, Topoisomerase IIα and MGMT

JIANG-BO QIN[1], HUI ZHANG[1], XIAO-CHUN WANG[2], YAN TAN[1] and XIAO-FENG WU[1]

[1]Department of Radiology, The First Clinical Medical College of Shanxi Medical University;
[2]Department of Medical Imaging, Shanxi Medical University, Taiyuan, Shanxi 030001, P.R. China

Received October 6, 2016; Accepted January 19, 2017

DOI: 10.3892/ol.2019.10656

**Abstract.** The present study aimed to investigate the value of diffusion-weighted imaging (DWI) combined with dynamic susceptibility contrast-enhanced (DSC) magnetic resonance imaging (MRI) scans in astrocytoma grading, and correlated MRI scan parameters of values of apparent diffusion coefficient (ADC) and relative cereberal blood volume (rCBV) with the immunohistochemical (IHC) indices of glial fibrillary acidic protein (GFAP), topoisomerase IIα (Topo IIα) and O 6-methylguanine-DNA methyltransferase (MGMT). A total of 123 patients with pathologically confirmed astrocytomas of differing grades underwent DWI and DSC scans. The values of the ADC and relative cerebral blood volume rCBV were compared with the grade II-IV astrocytomas. Receiver operating characteristic curves were used to compare astrocytoma grading efficiency of ADC, rCBV and the combination of the two values. The parameters of ADC and rCBV with GFAP, Topo IIα and MGMT indices were then correlated. The differences in ADC values were significant between the grades II, III and IV astrocytomas, and the rCBV values for grades II, III and IV were also significant. The combination of DWI and DSC demonstrated the highest values for area under curve in identifying grades II and III, and identifying grades III and IV, respectively. GFAP displayed a positive correlation with ADC and a negative correlation with rCBV. Topo IIα exhibited a negative correlation with ADC, and a positive correlation with rCBV. No correlation was observed between MGMT and ADC or rCBV. The combined application of DWI and DSC may increase astrocytoma grading accuracy. Values of ADC and rCBV exhibit certain correlations with IHC indices, and may predict degree of malignancy of astrocytoma.

*Correspondence to:* Dr Hui Zhang, Department of Radiology, The First Clinical Medical College of Shanxi Medical University, 85 Jiefang South Road, Yingze, Shanxi 030001, P.R. China
E-mail: zhanghui_mr@163.com

*Key words:* astrocytoma grading, dynamic susceptibility contrast-enhanced, diffusion weighted imaging, immunohistochemistry

## Introduction

Astrocytoma is the most common type of adult primary brain tumor (1,2), and accurate grading of this tumor is critical to prepare appropriate treatment and to evaluate the prognosis of the patient. Classical histological classification and malignancy grading are based on the criteria of the 2007 World Health Organization (WHO) classification of tumors of the central nervous system (3), and astrocytoma are classified into I-IV grades; grade I-II, benign: Grade III-IV, malignant. However, for patients treated without surgery, it is not possible to obtain a pathological grade. Additionally, grades of pathological diagnosis made from surgical resection samples may be underestimated due to tumoral heterogeneity.

Functional magnetic resonance imaging (MRI) scanning technologies, such as diffusion-weighted imaging (DWI), may provide data on tumor cell density and proliferation and serve as an important supplement to conventional MRI scans such as T1-weighted image (T1WI), T2-weighted image (T2WI), T2-fluid attenuated inversion recovery (FLAIR) scans (4-8). DWI may quantify the diffusion rate of extracellular water molecules, and the limited diffusion of water molecules in high-grade astrocytoma results in a low apparent diffusion coefficient (ADC) value. In addition, the astrocytoma grade is associated with the vasculature of the tumor, and may be reflected by relative cerebral blood volume (rCBV), thus guiding astrocytoma grading (8,9).

However, functional MRI scanning technology with DWI or DSC cannot incorporate all features of astrocytomas comprehensively. A previous study demonstrated that the accuracy of DWI or dynamic susceptibility contrast-enhanced (DSC) measurements in differentiating between grades of astrocytoma exhibited unsatisfactory consequences (4). For example, DWI has been revealed to increase diagnostic accuracy of astrocytoma grade, but a singular DWI-MRI scan cannot provide sufficient quantitative data concerning tumor structure (10). Additionally, previous studies have not investigated the associations between DWI- and DSC-MRI scans and immunohistochemical (IHC) indices.

In the present study, the efficacy of the combination of DWI- and DSC-MRI scans in astrocytoma grading, and the associations between these MRI scans and the

histologic indices of glial fibrillary acidic protein (GFAP), topoisomerase IIα (Topo IIα) and O 6-methylguanine-DNA methyltransferase (MGMT) were investigated. Histologic measurement of GFAP, Topo IIα and MGMT is widely used in evaluating the levels of tumor infiltration and proliferation, and has been demonstrated to correlate with tumor grade and prognosis (11-13). The main aim of the present study was to identify the accuracy of combined diagnostic techniques in differentiating between grades II-IV astrocytoma, and to predict astrocytoma malignancy through comparing histologic measurement of levels of GFAP, Topo IIα and MGMT.

## Materials and methods

*Ethical considerations*. The present study was approved by Shanxi Medical University review board. All manuscripts comply with the guidelines of the February 2006 consensus statement of the International Committee of Medical Journal Editors, and all patients provided written informed consent.

*Patient selection*. A total of 123 patients, 62 male and 61 female, with an age range between 25 and 77 years, and a mean age of 51.3±11.2 years, with histologically confirmed astrocytoma subsequent to surgical resection in The First Hospital of Shanxi Medical University between April 2010 and December 2015 were included. All patients underwent DWI, DSC and conventional MRI scans within 2 weeks prior to surgical resection. Pathological specimens were classified according to the WHO 2007 central nervous system tumor classification guidelines (3). Astrocytoma were grouped into low-grade astrocytoma, WHO grade II, 23 patients; anaplastic astrocytomas, WHO grade III, 44 patients; and glioblastoma multiforme, WHO grade IV, 56 patients.

*MRI acquisition*. MRI scans were performed using the General Electric (GE) SIGNA HDx 3.0 Tesla MR scanner with an 8-channel phased-array coil with a head and neck combination. All patients underwent conventional T1WI, T2WI, T2-FLAIR and DWI axial scanning, followed by DSC-MR perfusion scanning. DSC-MR perfusion images were captured by elbow vein bolus injection of gadopentetate dimeglumine (Magnevist®, Bayer Schering Pharma AG, Berlin, Germany) at a flow rate of 4.5 ml/s and a dose of 0.1 mmol/kg. Finally, conventional T1WI enhancement scanning was performed.

The scan protocol of each conventional MRI scan included: T1WI, with a repetition time (TR)/echo time (TE) of 1677/24 ms; T2WI, with a TR/TE of 6800/105 ms; T2-FLAIR, with a TR/TE of 8002/132 ms, a thickness of 6 mm, spacing of 1.2 mm between two adjacent images, a field of view (FOV) of 240x240 mm, matrix 320x256 mm, and number of excitations (NEX)=1. DWI scans used a spin echo/echo planar imaging sequence, a TR/TE of 5,000/74 ms, a thickness of 6 mm, spacing of 1.2 mm, FOV 240x240 mm, matrix 160x160 mm, and NEX=2; the diffusion coefficient of sensitivity was selected as 0.1000 s/mm$^2$. The parameters of the DSC MRI perfusion scans were as follows: TR/TE of 1500/14.5 ms, FOV of 240x255 mm, a matrix of 128x128 mm, a flip angle of 90˚ and a NEX=1. The elbow intravenous bolus injections of gadopentetate dimeglumine were administered with a flow rate of 4.5 ml/s, followed by injection of normal saline at the same flow rate.

*DWI and DSC images post-processing and analysis*. The original DWI and DSC maps were transmitted to an advanced workstation 4.4 to generate the ADC and rCBV maps, respectively. A total of three regions of interest (ROIs) in the tumor parenchyma region on the ADC map were selected, and ADC values were measured and averaged. ROI selection avoided the areas of hemorrhage, necrosis, cystic degeneration and larger vessel areas. A total of three ROIs at the tumor parenchyma on the rCBV maps were drawn to measure the rCBV values and averaged. The ROIs of the contralateral normal-appearing white matter (NAWM) were also drawn. The rCBV included in the present study was defined as the normalized rCBV value; rCBV value=the averaged rCBV value in parenchyma/the rCBV value in contralateral NAWM. The ADC and rCBV values were confirmed focus of the present study. A total of two blinded, independent radiologists performed the image analyses.

*Histopathology*. The specimens were paraffin embedded subsequent to 4% formalin fixation and buffered in PBS, and 1-$\mu$m sections were prepared for hematoxylin-eosin (HE) staining. Astrocytoma were histopathologically classified according to the 2007 WHO central nervous system classification criteria (3). The IHC indexes for GFAP, Topo IIα and MGMT were assessed. The tumor parenchyma underwent corresponding paraffin cuts and conventional dewaxing into water, and avidin-biotin complex (ABC) IHC staining was performed. The main reagents and instruments including GFAP, Topo IIα and MGMT monoclonal antibodies were supplied by Dako; Agilent Technologies, Inc. (Santa Clara, CA, USA), the ABC kit from Sigma-Aldrich Merck KGaA (Darmstadt, Germany), the DAB chromogenic agent from Sigma-Aldrich; Merck KGaA and the Digital Scan Scope case scanning system (Merck KGaA). The Aperio Digital Pathology image analysis system (Leica Microsystems GmbH, Wetzlar, Germany) and the software Cytoplasmic V2 (Leica Microsystems GmbH) were used to select richly stained tumor tissue sections. A total of three standard fields of vision were randomly selected and the average optical density was measured to compute an average for GFAP, Topo IIα and MGMT expression levels of cells.

*Statistical analysis*. The ADC and rCBV values of different grades of astrocytoma were compared using a two sample unpaired t-test analysis. ROC curves were used to assess the astrocytoma grading efficiency of ADC, rCBV and combined values of ADC and rCBV. Associations between the MRI parameters and the IHC indices of GFAP, Topo IIα and MGMT were analyzed using the Pearson correlation method. $P<0.05$ was considered to indicate a statistically significant difference.

## Results

*Comparisons of ADC and rCBV values among grade II-IV astrocytoma*. The DWI parameter value, ADC, and DSC parameter value, rCBV, of the tumoral parenchyma are illustrated in Table I. The ADC values in the grade II astrocytoma were significantly higher compared with the grade III astrocytoma (P=0.003). The rCBV values in the grade II astrocytoma were significantly lower compared with the grade III astrocytoma

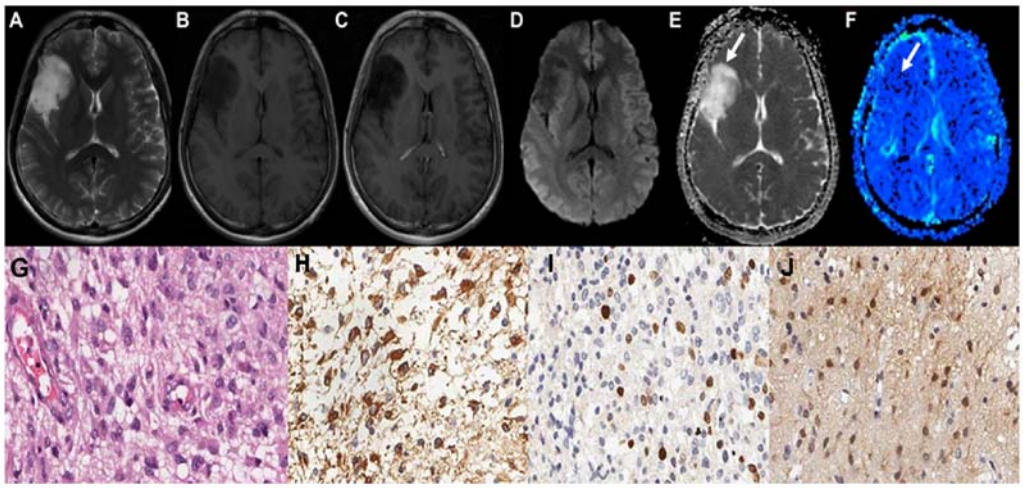


Figure 1. Right frontal lobe low-grade astrocytoma (Grade II) in a 25-year old male. (A) The right frontal lobe lesion exhibited irregular long T1 and (B) T2 signals. (C) Axial contrast-enhanced T1 weighted image revealed no significant enhancement. (D) Lesions displayed iso-low signal on the diffusion-weighted imaging map. (E) The apparent diffusion coefficient map displayed high signal (arrow), (F) The relative cerebral blood volume value was low in the tumor parenchyma (arrow). (G) Well-differentiated tumor cells with slight nuclear atypia were exhibited on a hematoxylin and eosin staining map. (H) High expression of glial fibrillary acidic protein in the cytoplasm. (I) A limited level of expression of topoisomerase IIα in the nucleus. (J) The O 6-methylguanine-DNA methyltransferase proteins demonstrated moderate expression levels in the cytoplasm and nucleus.

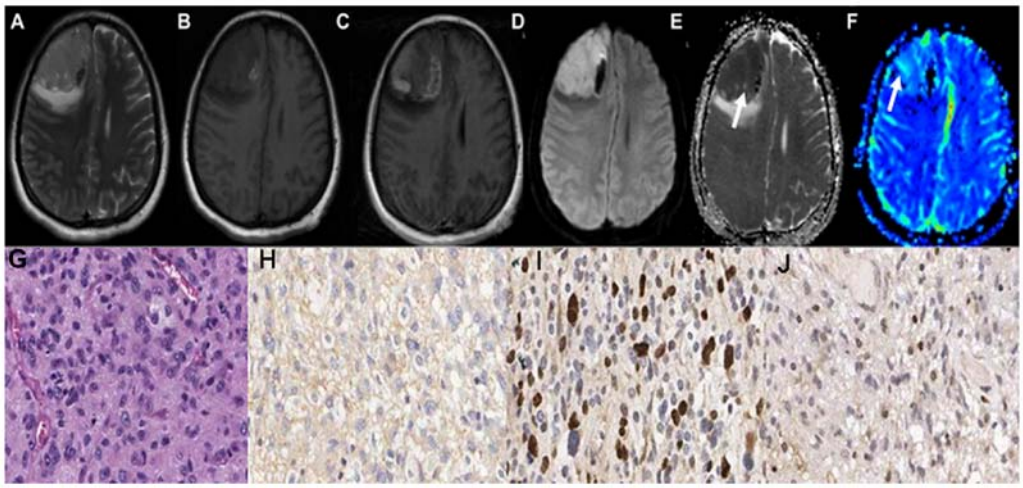


Figure 2. Right frontal lobe anaplastic astrocytoma (Grade III) in a 43-year-old female patient. (A) The right frontal lobe lesion exhibited a phymatoid isointense signal on T1 and (B) T2 WI. (C) Axial contrast-enhanced T1 WI revealed mild to moderate enhancement. (D) Lesions exhibited a hyper-intense signal on diffusion-weighted imaging map. (E) The apparent diffusion coefficient map displayed low signal in the tumor parenchyma (arrow). (F) The relative cerebral blood volume value was high in the tumor parenchyma (arrow). (G) hematoxylin and eosin staining map revealed moderately differentiated tumor cells with nuclear atypia. (H) Moderate glial fibrillary acidic protein expression level in the cytoplasm. (I) Moderate expression level of topoisomerase IIα in the nucleus. (J) The O 6-methylguanine-DNA methyltransferase proteins demonstrated a low to moderate expression level in the cytoplasm and nucleus. WI, weighted image.

(P=0.012). The ADC values in the grade III astrocytoma were significantly higher compared with the grade III astrocytoma (P=0.041). The rCBV values in the grade III astrocytoma were significantly lower compared with the grade IV astrocytoma (P=0.035).

The maps of the aforementioned conventional MRI scans of grade II astrocytoma are demonstrated in Fig. 1A-C. Grade II astrocytoma exhibited low signal on DWI sequence, and high ADC values, as illustrated in Fig. 1D and E. The parenchyma of grades II astrocytoma on the rCBV maps exhibited low signals, as illustrated in Fig. 1F-J demonstrate the HE staining map, IHC. GFAP map, IHC. Topo IIα map and IHC. MGMT map of grades II astrocytoma respectively. The conventional MRI scans of grade III astrocytoma are demonstrated in Fig. 2A-C. Grade III astrocytoma demonstrated high signal on DWI sequence, and the ADC values of the tumor parenchyma were lower, as illustrated in Fig. 2D and E. The parenchyma of grades III astrocytoma on the rCBV maps exhibited high signals, as illustrated in Fig. 2F-J demonstrate the HE staining map, IHC. GFAP map, IHC. Topo IIα map and IHC. MGMT map of grades III astrocytoma respectively. The conventional MRI scans of grade IV astrocytoma are demonstrated in Fig. 3A-C. Grade IV astrocytoma demonstrated the highest signal on the DWI maps, and the ADC values were the lowest between all of the astrocytoma grades, as illustrated in Fig. 3D and E. The grade IV astrocytoma on the rCBV map

Table I. Comparison of DWI and DSC parameters among grade II-IV astrocytoma.

| | Grade II vs. III | | | Grade III vs. IV | | |
|---|---|---|---|---|---|---|
| Parameters | Grade II (n=23) | Grade III (n=44) | P-value | Grade III (n=44) | Grade IV (n=56) | P-value |
| ADC | 1.299±0.294 | 0.929±0.170 | 0.003[a] | 0.929±0.170 | 0.790±0.176 | 0.041[a] |
| rCBV | 2.552±0.705 | 5.195±1.883 | 0.012[a] | 5.195±1.883 | 7.070±1.721 | 0.035[a] |

ADC, apparent diffusion coefficient; rCBV, relative cerebral blood volume; the units for ADC was $mm^2/s$. [a]Statistically significantly difference between 2 groups.

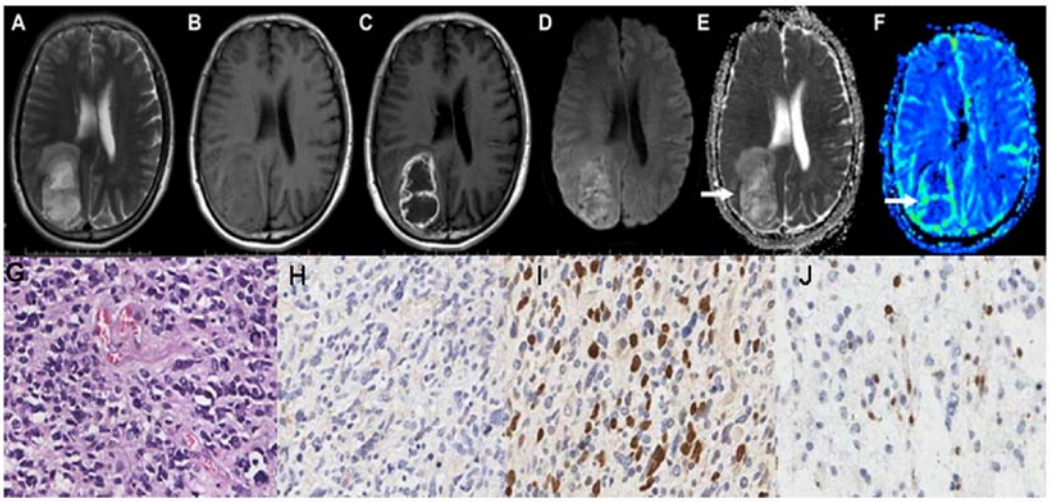


Figure 3. Right occipital lobe glioblastoma multiforme (Grade IV) in a 59-year-old male. (A) The cystic wall of the right occipital lobe lesion demonstrated a iso-intense signal on T1 and (B) T2WI, and the cystic fluid was hypo-intense on T1WI and hyper-intense on T2WI. (C) Axial contrast-enhanced T1W image exhibited marked enhancement of the cystic wall. (D) The cystic wall demonstrated a hyper-intense signal on diffusion-weighted imaging map. (E) The apparent diffusion coefficient value was low in the cystic wall (arrow). (F) The relative cerebral blood volume value was highest in the cystic wall (arrow). (G) Poorly differentiated tumor cells with remarkable nuclear atypia with nucleolar enlargement and increased karyokinesis were displayed on a hematoxylin and eosin staining map. (H) Low glial fibrillary acidic protein expression level in the cytoplasm. (I) High expression level of topoisomerase IIα in the nucleus. (J) The O 6-methylguanine-DNA methyltransferase proteins displayed low expression levels in the nucleus. WI, weighted image.

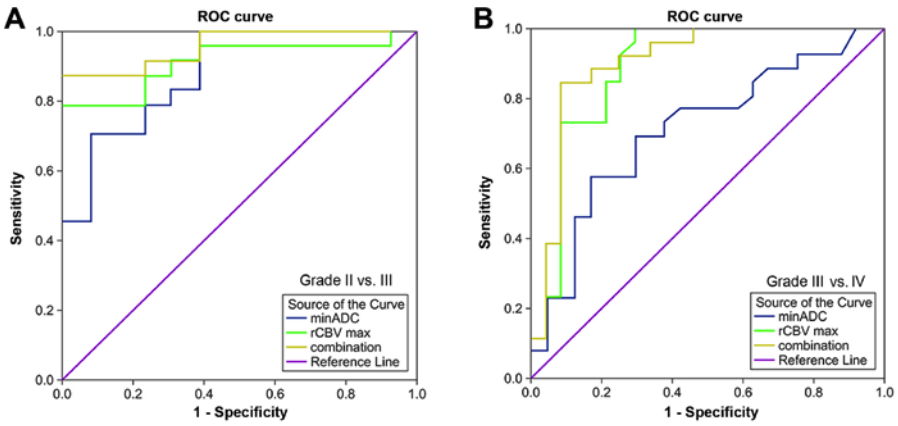


Figure 4. (A) ROC analysis of DWI, DSC and combined parameters in differentiating grade II and III astrocytomas; (B) ROC analysis of DWI, DSC and combined parameters in differentiating grade III and IV astrocytomas. ROC, receiver operating characteristic; DWI, diffusion-weighted imaging; DSC, dynamic susceptibility contrast-enhanced imaging; rCBV, relative cerebral blood volume; ADC, apparent diffusion coefficient.

demonstrated the highest signal, as illustrated in Fig. 3F-J demonstrate the HE staining map, IHC. GFAP map, IHC. Topo IIα map and IHC. MGMT map of grades IV astrocytoma respectively.

*ROC analysis of DWI, DSC and combined parameters in identifying grade II-III and III-IV astrocytoma*. ROC analysis of value of ADC, value of rCBV, and the combined value of ADC and rCBV in differentiating between grades II and III

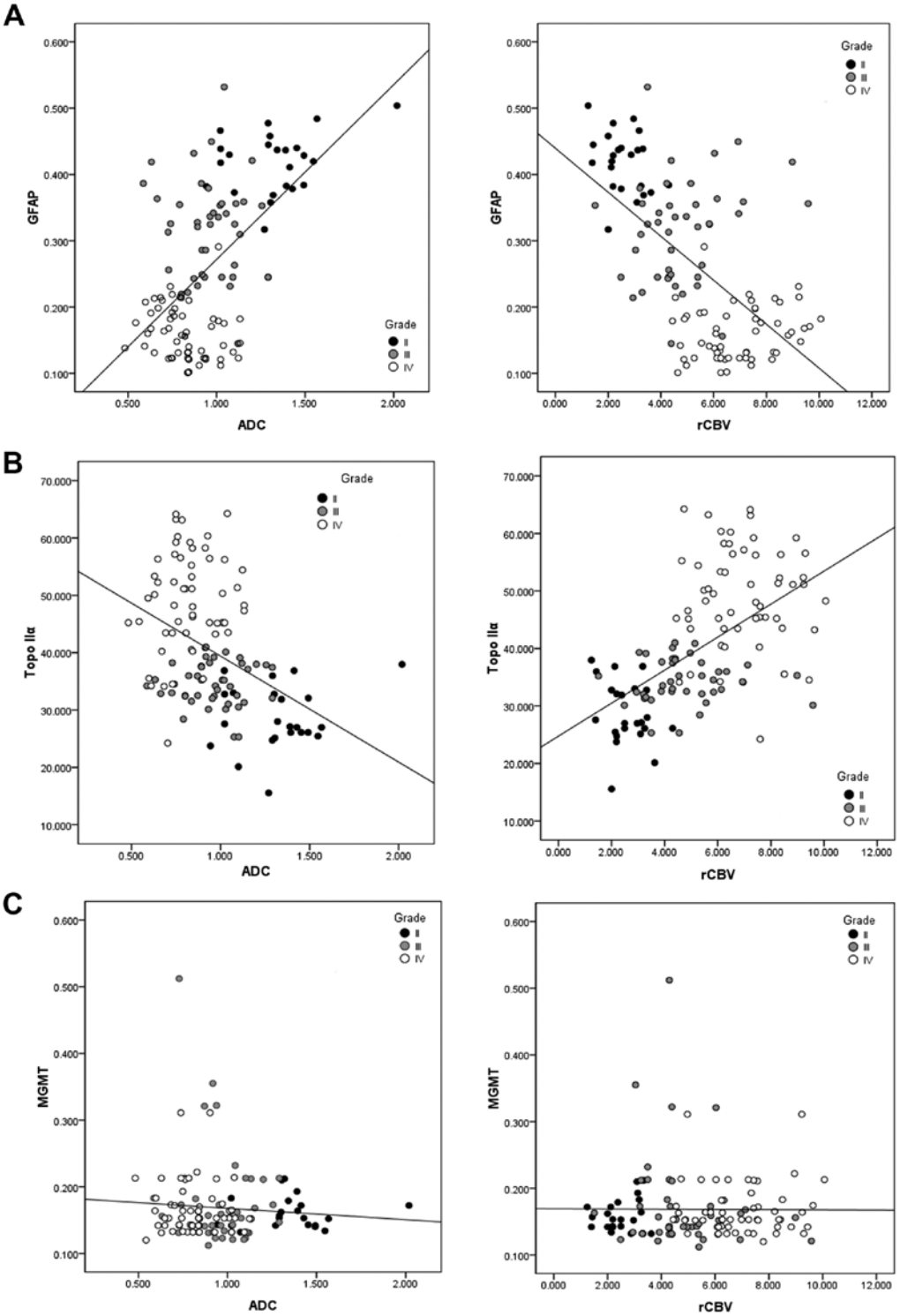


Figure 5. (A) Correlation analysis between GFAP and MRI parameters; (B) Correlation analysis between Topo IIα and MRI parameters; (C) Correlation analysis between MGMT and MRI parameters. MRI; magnetic resonance imaging; GFAP, glial fibrillary acidic protein; Topo IIα, topoisomerase IIα; MGMT, O 6-methylguanine-DNA methyltransferase.

astrocytoma was illustrated in Fig. 4A and Table II. The combined diagnostics method had the highest area under the curve (AUC), 0.958, in distinguishing between grades II and III astrocytoma, followed by rCBV, 0.913, and ADC, 0.885. ROC analysis of ADC, rCBV and the combined diagnostics method in differentiating between grades III and IV astrocytoma is demonstrated in Fig. 4B and Table II. The combined parameter had the highest AUC, 0.904, in distinguishing between grades III and IV astrocytoma, followed by rCBV, 0.889, and ADC, 0.712.

*Correlations between MRI parameters and IHC indices*. A positive correlation was exhibited between levels of GFAP and ADC (r=0.574, P<0.001), whilst a negative correlation was

Table II. Receiver operating characteristic analysis of diffusion-weighted imaging, dynamic susceptibility contrast-enhanced imaging and combined values in differentiating grade II-IV astrocytoma.

| | Grade II vs. III | | | | | Grade III vs. IV | | | | |
|---|---|---|---|---|---|---|---|---|---|---|
| Parameters | AUC | P-value | Cut-off value | Sensitivity (%) | Specificity (%) | AUC | P-value | Cut-off value | Sensitivity (%) | Specificity (%) |
| ADC | 0.885 | 0.034 | 1.021 | 70.8 | 92.9 | 0.712 | 0.035 | 0.783 | 57.7 | 83.3 |
| rCBV | 0.913 | 0.024 | 3.760 | 79.2 | 100 | 0.889 | 0.043 | 5.870 | 100 | 70.8 |
| Combined value | 0.958 | 0.001 | | 87.5 | 100 | 0.904 | 0.002 | | 84.6 | 91.7 |

ADC, apparent diffusion coefficient; rCBV, relative cerebral blood volume; AUC, areas under curves.

Table III. Correlation between the values of DWI/DSC and IHC parameters.

| MRI and IHC parameters | r-value | P-value |
|---|---|---|
| GFAP | | |
| ADC-GFAP | 0.574 | <0.001 |
| rCBV-GFAP | -0.610 | <0.001 |
| Topo IIα | | |
| ADC-Topo IIα | -0.435 | <0.001 |
| rCBV-Topo IIα | 0.571 | <0.001 |
| MGMT | | |
| ADC-MGMT | -0.082 | 0.364 |
| rCBV-MGMT | 0.024 | 0.790 |

P=DWI/DSC vs. IHC marker. IHC, immunohistochemistry; MRI, magnetic resonance imaging; GFAP, glial fibrillary acidic protein; Topo IIα, topoisomerase IIα; MGMT, O 6-methylguanine-DNA methyltransferase; ADC, apparent diffusion coefficient; rCBV, relative cerebral blood flow.

demonstrated between levels of GFAP and rCBV (r=-0.610, P<0.001; Fig. 5A). A negative correlation was demonstrated between levels of Topo IIα and ADC (r=-0.435, P<0.001; Fig. 5B), and a positive correlation was exhibited between levels of Topo IIα and rCBV (r=0.571, P<0.001; Fig. 5C). No correlation was observed between levels of MGMT and ADC (r=-0.082, P=0.364 or rCBV of the astrocytoma (r=0.024, P=0.790). These correlations between the MRI parameters and the IHC indices are summarized in Table III.

## Discussion

In the present study, the DWI and DSC parameters of different grade astrocytoma were compared and the potential of combing DWI and DSC data in astrocytoma grading was evaluated. In addition, the correlation between DWI and DSC parameters and IHC indices were examined. The results demonstrate that the ADC and rCBV data exhibited significant differences between the grades II-IV astrocytoma. Concurrently, the combined diagnostic method exhibited the highest accuracy in differentiating between grades II-IV astrocytoma. ADC and rCBV measurements demonstrated correlations with levels of GFAP and Topo IIα. No association between MRI parameters and levels of MGMT was observed.

Cells and subcellular structures limit the diffusion of water molecules (14), and ADC values can quantify this limited degree of diffusion. Thus, DWI can non-invasively assess tumor cell density (15-17). In the present study, there was a significant difference in ADC values of tumor parenchyma between grades II and III (P<0.05); this result is consistent with the findings of Lee *et al* (15), Kono *et al* (16) and Calli *et al* (18). These previous studies revealed that the ADC values of high-grade astrocytoma decreased significantly, and the DWI signal increased. Previous studies on DWI of gliomas examined the differences in ADC value between high-grade and low-grade gliomas, yet the present study explored the values of DWI in differentiating between grades II, III,

and IV astrocytoma. In the present study, the ADC value for grade IV astrocytoma was $0.790\pm0.176x10^{-3}$ $mm^2/s$, which was lower compared with the value revealed by Stadnik *et al*, $1.14x10^{-3}$ $mm^2/s$ (19). This difference may be associated with the selection of ROI in the tumor parenchyma.

Invasiveness and tumor growth are closely associated with neovascularization (20). Therefore, utilizing a rCBV map of MR perfusion images for the description of the characteristics of astrocytoma exhibits potential that an rCBV map may be able to evaluate the degree of angiogenesis. One study suggested that DSC-MR perfusion-weighted imaging serves a major role in the identification of high- and low-grade gliomas, and the rCBV values are significantly different (6). The aforementioned study is consistent with the results reported in the present study, in which grades II and IV were compared with grade III astrocytoma, and a statistically significant difference in rCBV values was revealed. The results of the present study are different from those reported in the study by Hakyemez *et al* (2), in which no significant difference as observed between grades III and IV; this may be due to the correction of the rCBV value with the contralateral NAWM in the present study.

The present study focused on examining whether the combined methods of ADC and rCBV measurements may improve efficiency in astrocytoma grading. This is the first study in which the combination of DWI and DSC MRI scanning may be used as a classifying instrument in the grading of astrocytoma. The combined diagnostic method increased the diagnostic power and had the highest AUC, 0.943, and highest sensitivity, 87.5%, compared with ADC and rCBV measurements alone, and a higher specificity, 100%, compared with ADC measurements in astrocytoma grading. Through the joint application of an arterial spin labeling technique and ADC values to glioma grading, Kim *et al* (21) also concluded that the use of multiple techniques improves the diagnostic accuracy of gliomas, serving as an effective supplement to conventional MRI techniques. Hilario *et al* (22) demonstrated that the combination of minimum ADC and maximum rCBV measurements improves the diagnostic accuracy of glioma grading. However, these previous studies focus on gliomas as the type of cancer studied, which covers several types of brain tumor. There have been fewer reports investigating astrocytoma grading which apply DWI and DSC imaging. In the present study, the range was narrowed to astrocytoma from gliomas, which may provide increased precision for preoperative astrocytoma grading systems, and generate data pertinent for decisions concerning treatments .

GFAP is an intermediate filament cytoskeleton protein which is expressed specifically by the gliocyte (11). Ilhan-Mutlu *et al* (23) reported that a decreased GFAP expression was associated with an increasing malignancy grade in gliomas. In the present study, a significant negative correlation between GFAP and rCBV ($r=-0.610$, $P<0.001$), and a positive correlation between GFAP and ADC ($r=0.574$, $P<0.001$) was revealed. The decreased GFAP expression level correlated with the aggressiveness and malignancy of astrocytoma, whilst rCBV and ADC levels reflected the vasculation and cell density, which were associated with the malignancy of tumors, which many be potential explanations for the above correlation.

It was suggested that Topo IIα was associated with cellular proliferation (24). In the present study, it was demonstrated that Topo IIα was negatively correlated with ADC ($r=-0.435$, $P<0.001$), and positively correlated with rCBV ($r=0.571$, $P<0.001$). ADC reflects the cell density of tumor, which may explain the correlation between Topo IIα and ADC. Therefore, ADC may reveal the Topo IIα expression levels, to predict the malignancy of astrocytoma. In addition, it was revealed that rCBV also reflected the levels of Topo IIα expression (25). Further studies are required to examine the internal association between rCBV and Topo IIα expression.

MGMT promoter methylation reflects the sensitivity of chemotherapeutic drugs (temozolomide) to astrocytoma patients. The existence of an association between expression levels of MGMT protein and MGMT promoter methylation remains unknown (26). In the present study, no correlation was observed between values of ADC and rCBV and MGMT protein expression. As aforementioned, this association requires additional study.

The present study included certain limitations. Firstly, cystic-solid tumors may possess thin cystic wall tissues, and the selected ROIs of ADC or rCBV may contain a portion of normal brain parenchyma outside the cystic wall of the tumor (27). This may lead to inaccurate assessment of ADC and rCBV values to tumor cell proliferation and vascular proliferation. Secondly, pathological misdiagnosis may occur due to sampling errors caused by tumor heterogeneity, particularly for malignant astrocytoma: For example, the tumor samples may contain grades II and III astrocytoma cells. In addition, manually drawing ROIs is a tedious procedure and may incur personal error. Finally, the investigation did not involve analysis of prognoses, which should be explored in future studies.

In conclusion, the present study demonstrated that the combination of DWI and DSC measurements may improve the accuracy of astrocytoma grading. The DWI and DSC measurements which exhibit correlations with IHC indices of GFAP and Topo IIα may be useful biomarkers in predicting the levels of malignancy in astrocytoma.

**Acknowledgements**

Not applicable.

**Funding**

The present study was supported by grants from the National Natural Science Foundation of China (grant nos. 81471652, 81771824 and 81701681), the Precision Medicine Key Innovation Team Project (grant no. YT1601), the Social Development Projects of Key R&D Programs in the Shanxi Province (grant no. 201703D321016) and the Natural Science Foundation of Shanxi Province (grant no. 201601D021162).

**Availability of data and materials**

The datasets used or analyzed during the current study are available from the corresponding author on reasonable request.

**Authors' contributions**

HZ proposed the notion of the present study and interpreted the patient data. JQ performed the majority of the experiments

and was a major contributor in writing the manuscript. XWa analyzed the data and designed the figures. YT and XWu collected and managed the samples. All authors read and approved the final manuscript for publication.

**Ethics approval and consent to participate**

The present study was approved by Shanxi Medical University review board. All manuscripts comply with the guidelines of the February 2006 consensus statement of the International Committee of Medical Journal Editors, and all patients provided written informed consent prior to their inclusion within the study.

**Consent for publication**

All patients provided written informed consent for the publication of their data.

**Competing interests**

The authors declare that they have no competing interests.

**References**


1. Warmuth C, Gunther M and Zimmer C: Quantification of blood flow in brain tumors: Comparison of arterial spin labeling and dynamic susceptibility-weighted contrast-enhanced MR imaging. Radiology 228: 523-532, 2003.
2. Hakyemez B, Erdogan C, Ercan I, Ergin N, Uysal S and Atahan S: High-grade and low-grade gliomas: Differentiation by using perfusion MR imaging. Clin Radiol 60: 493-502, 2005.
3. Louis DN, Ohgaki H, Wiestler OD, Cavenee WK, Burger PC, Jouvet A, Scheithauer BW and Kleihues P: The 2007 WHO classification of tumours of the central nervous system. Acta Neuropathol 114: 97-109, 2007.
4. Hirai T, Murakami R, Nakamura H, Kitajima M, Fukuoka H, Sasao A, Akter M, Hayashida Y, Toya R, Oya N, *et al*: Prognostic value of perfusion MR imaging of high-grade astrocytomas: Long-term follow-up study. AJNR Am J Neuroradiol 29: 1505-1510, 2008.
5. Bulakbasi N, Kocaoglu M, Farzaliyev A, Tayfun C, Ucoz T and Somuncu I: Assessment of diagnostic accuracy of perfusion MR imaging in primary and metastatic solitary malignant brain tumors. AJNR Am J Neuroradiol 26: 2187-2199, 2005.
6. Sadeghi N, D'Haene N, Decaestecker C, Levivier M, Metens T, Maris C, Wikler D, Baleriaux D, Salmon I and Goldman S: Apparent diffusion coefficient and cerebral blood volume in brain gliomas: Relation to tumor cell density and tumor microvessel density based on stereotactic biopsies. AJNR Am J Neuroradiol 29: 476-482, 2008.
7. Prager AJ, Martinez N, Beal K, Omuro A, Zhang Z and Young RJ: Diffusion and perfusion MRI to differentiate treatment-related changes including pseudoprogression from recurrent tumors in high-grade gliomas with histopathologic evidence. AJNR Am J Neuroradiol 36: 877-885, 2015.
8. Xiao HF, Chen ZY, Lou X, Wang YL, Gui QP, Wang Y, Shi KN, Zhou ZY, Zheng DD, Wang DJ and Ma L: Astrocytic tumour grading: A comparative study of three-dimensional pseudocontinuous arterial spin labelling, dynamic susceptibility contrast-enhanced perfusion-weighted imaging, and diffusion-weighted imaging. Eur Radiol 25: 3423-3430, 2015.
9. Leu K, Enzmann DR, Woodworth DC, Harris RJ, Tran AN, Lai A, Nghiemphu PL, Pope WB, Cloughesy TF and Ellingson BM: Hypervascular tumor volume estimated by comparison to a large-scale cerebral blood volume radiographic atlas predicts survival in recurrent glioblastoma treated with bevacizumab. Cancer Imaging 14: 31, 2014.
10. Le Bihan D: Apparent diffusion coefficient and beyond: What diffusion MR imaging can tell us about tissue structure. Radiology 268: 318-322, 2013.
11. Elobeid A, Bongcam-Rudloff E, Westermark B and Nister M: Effects of inducible glial fibrillary acidic protein on glioma cell motility and proliferation. J Neurosci Res 60: 245-256, 2000.
12. Faria MH, Goncalves BP, do Patrocinio RM, de Moraes-Filho MO and Rabenhorst SH: Expression of Ki-67, topoisomerase IIalpha and c-MYC in astrocytic tumors: Correlation with the histopathological grade and proliferative status. 26: 519-527, 2006.
13. Christmann M, Nagel G, Horn S, Krahn U, Wiewrodt D, Sommer C and Kaina B: MGMT activity, promoter methylation and immunohistochemistry of pretreatment and recurrent malignant gliomas: A comparative study on astrocytoma and glioblastoma. Int J Cancer 127: 2106-2118, 2010.
14. Kwee TC, Galbán CJ, Tsien C, Junck L, Sundgren PC, Ivancevic MK, Johnson TD, Meyer CR, Rehemtulla A, Ross BD and Chenevert TL: Comparison of apparent diffusion coefficients and distributed diffusion coefficients in high-grade gliomas. J Magn Reson Imaging 31: 531-537, 2010.
15. Lee EJ, Lee SK, Agid R, Bae JM, Keller A and Terbrugge K: Preoperative grading of presumptive low-grade astrocytomas on MR imaging: Diagnostic value of minimum apparent diffusion coefficient. AJNR Am J Neuroradiol 29: 1872-1877, 2008.
16. Kono K, Inoue Y, Nakayama K, Shakudo M, Morino M, Ohata K, Wakasa K and Yamada R: The role of diffusion-weighted imaging in patients with brain tumors. AJNR Am J Neuroradiol 22: 1081-1088, 2001.
17. Yamasaki F, Kurisu K, Satoh K, Arita K, Sugiyama K, Ohtaki M, Takaba J, Tominaga A, Hanaya R, Yoshioka H, *et al*: Apparent diffusion coefficient of human brain tumors at MR imaging. Radiology 235: 985-991, 2005.
18. Calli C, Kitis O, Yunten N, Yurtseven T, Islekel S and Akalin T: Perfusion and diffusion MR imaging in enhancing malignant cerebral tumors. Eur J Radiol 58: 394-403, 2006.
19. Stadnik TW, Chaskis C, Michotte A, Shabana WM, van Rompaey K, Luypaert R, Budinsky L, Jellus V and Osteaux M: Diffusion-weighted MR imaging of intracerebral masses: Comparison with conventional MR imaging and histologic findings. AJNR Am J Neuroradiol 22: 969-976, 2001.
20. Ueda M, Terai Y, Kumagai K, Ueki K, Yamaguchi H, Akise D and Ueki M: Vascular endothelial growth factor C gene expression is closely related to invasion phenotype in gynecological tumor cells. Gynencol Oncol 82: 162-166, 2001.
21. Kim HS and Kim SY: A prospective study on the added value of pulsed arterial spin-labeling and apparent diffusion coefficients in the grading of gliomas. AJNR Am J Neuroradiol 28: 1693-1699, 2007.
22. Hilario A, Ramos A, Perez-Nuñez A, Salvador E, Millan JM, Lagares A, Sepulveda JM, Gonzalez-Leon P, Hernandez-Lain A and Ricoy JR: The added value of apparent diffusion coefficient to cerebral blood volume in the preoperative grading of diffuse gliomas. AJNR Am J Neuroradiol 33: 701-707, 2012.
23. Ilhan-Mutlu A, Wagner L, Widhalm G, Wöhrer A, Bartsch S, Czech T, Heinzl H, Leutmezer F, Prayer D, Marosi C, *et al*: Exploratory investigation of eight circulating plasma markers in brain tumor patients. Neurosurg Rev 36: 45-56, 2013.
24. Kimura F, Okayasu I, Kakinuma H, Satoh Y, Kuwao S, Saegusa M and Watanabe J: Differential diagnosis of reactive mesothelial cells and malignant mesothelioma cells using the cell proliferation markers minichromosome maintenance protein 7, geminin, topoisomerase II alpha and Ki-67. Acta Cytol 57: 384-390, 2013.
25. Maia AC Jr, Malheiros SM, da Rocha AJ, da Silva CJ, Gabbai AA, Ferraz FA and Stávale JN: MR cerebral blood volume maps correlated with vascular endothelial growth factor expression and tumor grade in nonenhancing gliomas. AJNR Am J Neuroradiol 26: 777-783, 2005.
26. Felsberg J, Thon N, Eigenbrod S, Hentschel B, Sabel MC, Westphal M, Schackert G, Kreth FW, Pietsch T, Löffler M, *et al*: Promoter methylation and expression of *MGMT* and the DNA mismatch repair genes *MLH1*, *MSH2*, *MSH6* and *PMS2* in paired primary and recurrent glioblastomas. Int J Cancer 129: 659-670, 2011.
27. Svolos P, Kousi E, Kapsalaki E, Theodorou K, Fezoulidis I, Kappas C and Tsougos I: The role of diffusion and perfusion weighted imaging in the differential diagnosis of cerebral tumors: A review and future perspectives. Cancer Imaging 14: 20, 2014.